JOURNAL OF CATALYSIS 98, 392–400 (1986)

Crystallite Size Effects in Nickel Catalysts: Cyclohexane Dehydrogenation and Hydrogenolysis

P. H. DESAI[1] AND J. T. RICHARDSON[2]

Department of Chemical Engineering, University of Houston, University Park, Houston, Texas 77004

Received January 10, 1985; revised October 31, 1985

Crystallite size dependence of cyclohexane dehydrogenation and hydrogenolysis has been studied over silica-supported nickel catalysts. The samples were freshly prepared and sintered catalysts, produced by homogeneous precipitation–deposition and ranging from 25 to 40 wt% Ni on SiO_2. Crystallite size distributions were determined from magnetization data. Other experimental measurements, such as hydrogen chemisorption and catalytic kinetics, were made in the same cell in order to provide *in situ* precision. Average crystallite sizes varied from 2 to 4 nm and critical differences were found in this region. Areal rates for dehydrogenation more than doubled, whereas cyclohexane hydrogenolysis decreased by a factor of 5. These findings were shown to be consistent with a model wherein dehydrogenation occurs on crystal face sites and hydrogenolysis on edge positions. Benzene hydrogenolysis followed the same pattern as dehydrogenation, suggesting that common intermediates are involved.

INTRODUCTION

Supported metal catalysts are designed to expose as much metal surface as possible. Dispersing metal on a support creates very small crystallites such that surface-to-volume ratios are high. Thus activity is directly proportional to metal surface area, but only in cases where the surface rate is invariable with crystallite size. Where this is not true, crystallite size becomes important in both activity and selectivity patterns.

Boudart (*1*) classified surface reactions into two general groups—structure insensitive or facile and structure sensitive or demanding. Facile reactions usually involve only single-point adsorption. Metal dispersion, concentration or support have no effect on areal activity (rate per unit surface area). Demanding reactions require multiple bonding with specific geometrical surface groups. Areal rates vary with dispersion or support.

Van Hardeveld and co-workers (*2, 3*) provided a model for crystallite size effects in their work on surface sites in cubo-octahedra, taken as the best approximation for small crystallites. Five types of sites were identified in a regular cubo-octahedron: sites on (1) hexagonal planes (111), (2) square planes (100), (3) edges between (111) and (100) planes, (4) edges between two (111) planes, and (5) corners.

Face atoms of type (1) and (2) have high coordination (9 and 8, respectively) and increase in concentration as the crystallite size increases. Edge sites have lower coordination (7 each) and, together with corner sites, decrease as the size increases. Figure 1 shows the rapid changes in the fraction of different surface types as the crystallite size increases through the range most encountered in catalysis.

Bond (*4*) used this model to demonstrate that reactions requiring low-coordination sites follow a positive intrinsic factor (i.e., decrease in areal rate with increasing size). Conversely, large coordination sites exhibit negative intrinsic factors. Possible reasons for differences in reactivity may be found in

[1] Present address: Akzo Chemie America, Catalyst Division, Pasadena, Tex. 77507.

[2] To whom enquires should be addressed.

0021-9517/86 $3.00

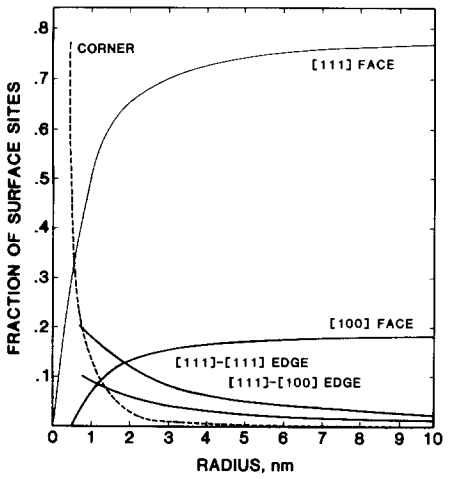

FIG. 1. Surface concentration of cubo-octahedron sites.

later concepts based on the symmetry and occupancy of *d*-orbitals emerging from different faces (*5*). Thus energetic and stereo factors in bonding of a surface atom with a molecule are influenced by the environment of the surface.

In reality the crystallites are closer to imperfect cubo-octahedra. Incomplete planes on faces generate step and kink sites together with associated edge and corner atoms. Possibility of size-dependent strain defects also exists as an additional complication (*6*). Nevertheless, the qualitative features shown in Fig. 1 provide a useful model for the rationalization of crystallite size effects.

A number of experimental studies have been reported in recent literature (*7–25*). In most of these, catalytic rates were measured in conventional kinetic equipment and related to size and/or surface area, *determined independently*. Techniques such as electron microscopy, X-ray diffraction, and magnetic measurements were used for size determination and some form of selective chemisorption for surface area. These methods require separate loading and activation of the sample in an apparatus distinctly different from that used in kinetic measurement. In most cases, it is freshly reduced catalyst that is characterized and related to activity. These procedures are highly uncertain, since there is sufficient reason to suspect that the state of the working surface is not the same as that seen for fresh catalyst in separate equipment.

Possible reasons for these differences are as follows:

(1) Extent of reduction and corresponding crystallite size (and distribution) are strongly dependent on temperature, rate of heating, hydrogen flow rate, and geometry of the apparatus (*26*). It is extremely difficult to maintain these conditions exactly the same in different samples. The best compromise is prereduction with some form of passivation such that less critical activation is sufficient, but even this introduces doubts due to different handling procedures.

(2) The working surface may develop only after deactivation of the most active sites during the early part of the process, possibly due to poisoning or irreversible adsorption of intermediates (*27*). Initial areas do not represent the active surface even in a proportional manner, since rate of deactivation or site development may also vary with size. One approach is to use pulse reactors, together with titration techniques (*27*), but simple kinetic interpretation is sacrificed.

(3) Crystallite size may increase during reaction due to reactive growth. Such phenomena have been observed in methanation studies (*28*). Characterizing the sample immediately after rate measurement is a solution, but handling procedures cast doubt on accuracy and relevency.

It is not surprising that in catalysis it is much more common to find differences than similarities. Identification of facile or structure insensitive reactions is an extremely difficult task. A solution to these problems is to make all measurements at the same time with *in situ* techniques. This ideal procedure is almost impossible to realize because of specific demands for each technique. Accordingly, the next best ap-

proach is to make all measurements in the same sample cell. In this way, the catalyst is identical for all measurements, providing procedural steps are controlled to minimize possible changes.

We have developed methods that accomplish these objectives for reduced nickel catalysts (*29–31*). A single tube serves as reactor, magnetometer cell, and chemisorption sample holder. With measurements of activity/selectivity, crystallite size distributions and hydrogen chemisorption possible on the same catalyst bed, uncertainties due to differences in activation and deactivation are eliminated and accurate areal rate–crystallite size correlations are possible.

We are pursuing this approach for a number of reactions over nickel, both to confirm previous speculations and to demonstrate new relationships. This report presents results for cyclohexane dehydrogenation/hydrogenolysis. Previous work by others have suggested that cyclohexane dehydrogenation increases with crystallite size whereas hydrogenolysis decreases (*15, 19*). In view of the importance of this effect in explaining selectivity factors in catalytic reforming, precise and accurate confirmation is both worthwhile and necessary.

This work not only substantiates these previous indications but also demonstrates that hydrogenolysis of benzene increases with larger crystallites, adding further complexity to the network of reactions.

EXPERIMENTAL

In situ sample cell. The sample cell shown in Fig. 2 was used for kinetic, magnetic, and chemisorption measurements, with reduction and sintering carried out on the same sample. Constructed of quartz with appropriate high-vacuum fittings, this cell allows for gas flow-through. The sample is approximately 0.066 to 0.165 g of catalyst packed into a bed, 1 cm in length. These dimensions are constrained by requirements of the magnetic coils. Quartz wool packing fills void space in the tube and

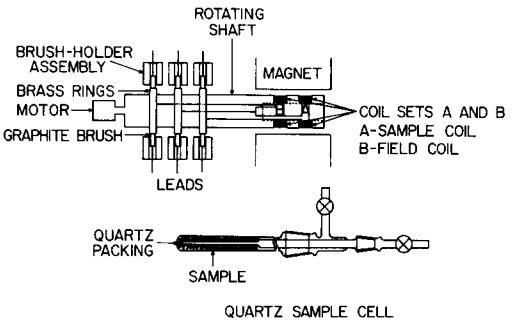

FIG. 2. Sample cell and magnetometer.

serves as both filling material and support for the sample. The ends of the valve fittings are attached with Cajon connectors to the various systems—kinetic, magnetic, and chemisorption.

Kinetic apparatus. Reduction, sintering, and kinetic measurements were made in the flow apparatus. Reduction was at 673 K in hydrogen flowing at 90–120 cm^3/min for 20 h. Sintering was carried out in helium between 873 and 973 K for 20 h. This procedure was adopted to increase crystallite size within the range of greatest sensitivity, as shown in Fig. 1.

Cyclohexane dehydrogenation–hydrogenolysis measurements were made with an integral microreactor system. Hydrogen was saturated with cyclohexane vapor at 298 K. Cyclohexane partial pressure was 0.13 atm with the remainder hydrogen. The total feed flow rate was adjusted to give space times up to 2.10×10^{-3} min. Gas sampling valves injected pulses into a Gow Mac Chromatograph Series 550 for feed and product analysis. The column was a 25 wt% Silicone DC550 on Celite 545 solid support in a 6-ft. $\frac{1}{4}$-in.-o.d. copper tube. The detector output was integrated to give the fraction of cyclohexane converted to benzene and C_1 products.

Magnetometer. The rotating magnetometer, shown in Fig. 2, has been described in detail elsewhere (*26*). Measurements of magnetization versus applied field were made up to 11 kOe and interpreted to give crystallite size distributions with computa-

TABLE 1

Physical Properties of Unreduced Catalysts

Catalyst	Total Ni %	BET surface area (m^2/g)
2	25	284
4	31	251
7	34	250
6	36	200
9	40	166

tional procedures described previously (*31*).

Chemisorption measurements. A Micromeritics Surface Area Analyzer was used for hydrogen chemisorption measurements. In each case an isotherm of the volume adsorbed at 298 K versus pressure was obtained up to 1 atm. Monolayer coverage was calculated by extrapolating the linear high-pressure region to zero pressure. The assumed hydrogen nickel stoichiometry was 1 : 1 with a nickel atom area of 0.065 nm^2.

Catalyst preparation. Catalysts were prepared by the homogeneous deposition method reported by Richardson and Dubus (*26*). Required amounts of nickel nitrate were dissolved in water and slurried with silica (Cab-O-Sil HS5, 275 m^2/g) at 363 K. Addition of urea at 363 K initiated uniform deposition of nickel hydrosilicate for times from 250 to 900 min. The suspension was cooled, filtered, washed, and dried at 939 K for 16 h. The dry catalyst was then crushed and seived to less than 60 mesh (250 μm).

Total nickel content was determined by a colorimetric method as described by Linsen (*32*). Nitrogen BET surface areas were measured with the Micromeretics Model 2100 D. Physical properties of reduced catalysts are reported in Table 1.

Experimental procedure. After reduction at 673 K in hydrogen, the catalyst was cleaned in helium at 698 K and 60–80 cm^3/min for 1 h. The cell was cooled to room temperature with helium flowing. Magnetization and chemisorption measurement were then made with the appropriate apparatus.

The cell was reconnected to the kinetic apparatus and the product distribution obtained for contact times up to 2×10^{-3} min at 573, 598, and 623 K.

In a selected number of cases, magnetization and chemisorption measurements were made after the reaction sequence to ensure that no reactive growth or surface area loss occurred.

The catalyst was then sintered in helium at temperatures between 873 and 973 K for 20 h in order to increase the crystallite size. Broadening of the distribution was found to accompany this growth. The sequence of magnetization, chemisorption, and kinetic measurement were repeated. A final sintering at 1093 K in helium for 20 h was necessary in order to obtain the saturation magnetization needed for calculation of the extent of reduction and crystallite size distributions. Replicate sample studies gave a precision for each measurement of better than 5%.

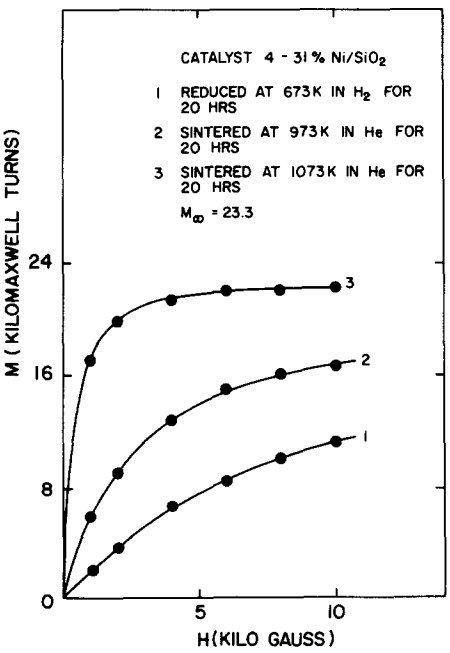

FIG. 3. Magnetization curves for Catalyst No. 4.

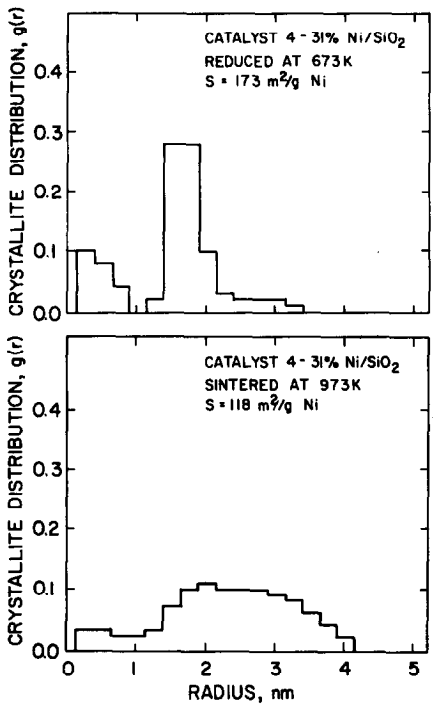

FIG. 4. Crystallite size distributions of Catalyst No. 4.

RESULTS AND DISCUSSION

Figures 3 through 8 show typical results for measurements and computations on Catalyst No. 4—31% Ni/SiO_2. Figure 4 gives magnetization curves after reduction and cleaning at 673 K, after sintering at 973 K, and final sintering at 1073 K. Crystallite size distributions, shown in Fig. 4, demonstrate typical results. The freshly reduced catalyst has small crystallites in the 0.2- to 0.8-nm range. A second group is found from 1.1 to 3.4 nm. The distribution is relatively narrow with a volume average radius of 1.95 nm. Sintering broadens the distribution with an average radius of 2.85 nm, only a 50% increase but in a critical range. The surface areas in Fig. 4 are calculated from the distribution.

Hydrogen adsorption isotherms are shown in Fig. 5. As usually found for dispersed nickel catalysts, the linear part of the curve shows no tendency to saturate. This uptake is reversible, easily desorbed, and may originate from any number of plausible reasons (*32*). Conclusions, based on many studies of this nature, lead us to believe that extrapolation is the best procedure to determine the monolayer. If this is not true, corrections will need to be made to all derived values, but the general trends as developed later in the discussion are still valid.

These extrapolated chemisorbed volumes were adjusted with nickel concentration and degree of reduction from saturation magnetization values to give a measured surface area per gram of reduced nickel. Comparing the results in Fig. 5 with those in Fig. 4 calculated from the measured crystallite size distributions, it may be seen that only 79 and 39% of the nickel surface is available for chemisorption. We call this factor "accessibility" and have addressed it in detail in a previous communication (*30*). An accessibility of less than one is believed to originate in pore trapping of crystallites or through interaction with

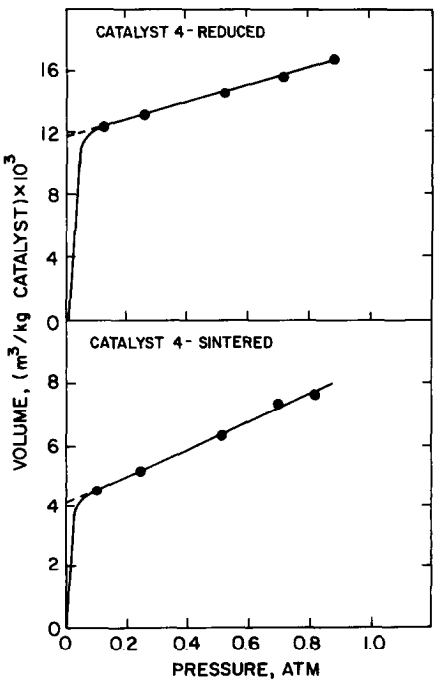

FIG. 5. Hydrogen chemisorption isotherms for Catalyst No. 4. Measured S_{Ni}: reduced, 136 m^2/g Ni; sintered, 46.2 m^2/g Ni.

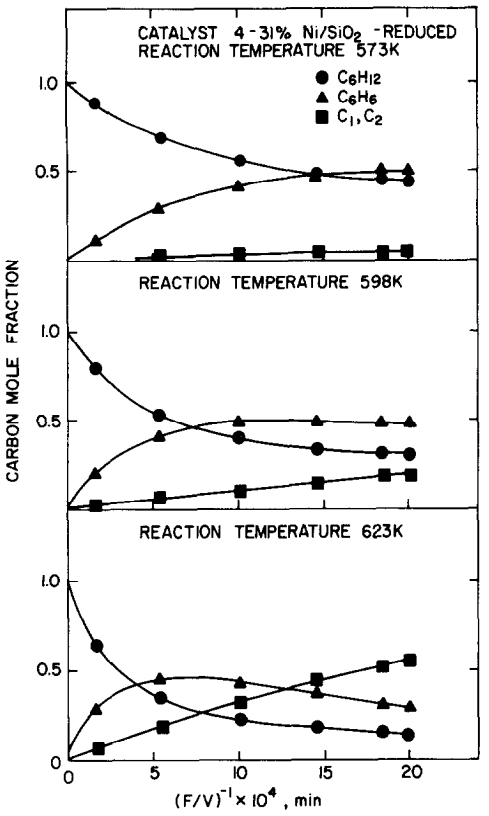

FIG. 6. Product distributions for Catalyst No. 4—reduced.

the support. Thermal treatment, as in sintering, merely aggravates the effect. Precise values for each sample used here are given in Ref. (*30*).

Although of interest, these phenomena are not pertinent in the research reported here. It should be noted, however, that in all subsequent discussion, surface areas measured from the hydrogen chemisorption are used to calculate areal rates whereas average radii determined from the crystallite size distributions are used to characterize the crystallite size.

Figures 6 and 7 show product distributions for the same sample in the reduced and sintered state. Three temperatures, 573, 598, and 623 K apply in each case. Three qualitative features result from these curves. First, products of hydrogenolysis are minor at 573 K but increase considerably at 623 K, indicating a high temperature coefficient. Second, benzene passes through a maximum, indicating that benzene hydrogenolysis has a significant rate. Finally, the shape of the C_1, C_2 curve is concave down for smaller crystallite sizes, whereas it becomes concave up for larger sizes. Increasing crystallite size presumably promotes benzene hydrogenolysis more than cyclohexane.

A reaction scheme suggested by these observations is shown in Fig. 8. Calculated equilibrium constants for cyclohexane dehydrogenation at the three temperature are 6.62, 46.4, and 280, respectively. Although the reverse benzene hydrogenation is significant at 573 K it becomes increasingly less so at higher temperature.

Kinetic interpretation of the network in Fig. 8 is difficult for any but simple-order rate expressions. Previous workers (*33–35*) found mostly first-order and zero-order ap-

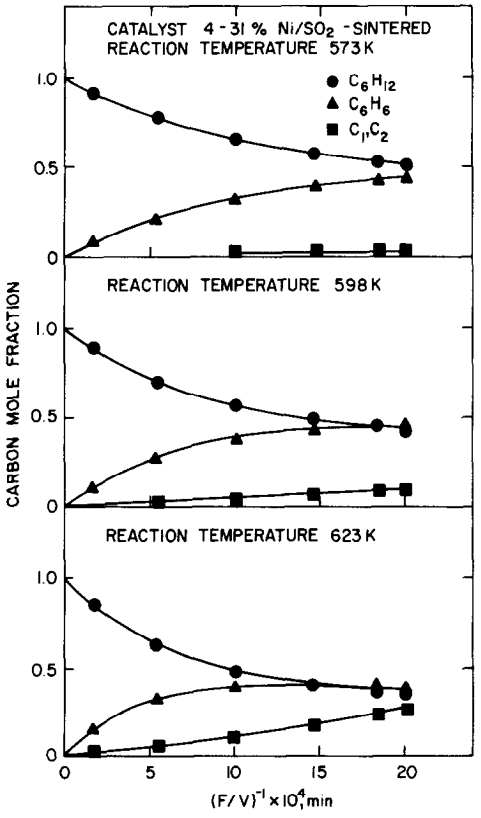

FIG. 7. Product distributions for Catalyst No. 4—sintered.

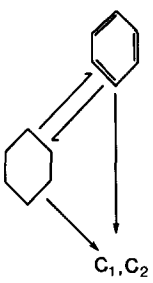

FIG. 8. Reaction network.

proximations for cyclohexane dehydrogenation and benzene hydrogenation, respectively. Benzene hydrogenolysis was reported as first-order also (*36*). However, cyclohexane disappearance in Figs. 6 and 7 do not follow first-order but suggest Langmuir–Hinshelwood, product inhibition and/or reversibility. These complexities make kinetic fitting of these data tenuous. We prefer a more direct use of observed rates, converted to areal values. Only data at 623 K were used, partly because benzene hydrogenation is insignificant at this temperature and also because precision of hydrogenolysis rate measurement is better.

Initial rates of benzene and C_1, C_2 appearance were used to calculate the rate of cyclohexane dehydrogenation and hydrogenolysis under reaction conditions (cyclohexane partial pressure of 0.13 atm, excess hydrogen). Rate of benzene hydrogenolysis was determined by first calculating the order of cyclohexane disappearance (usually between 2 and 2.5), using this to find the rate of cyclohexane dehydrogenation (or benzene production) at a standard condition (benzene partial pressure of 0.05 atm), and then using the observed rate of benzene appearance or disappearance at this point to give the rate of benzene hydrogenolysis. If the implied assumption that cyclohexane concentration does not influence benzene hydrogenolysis is valid, then this is a legitimate way to compare relative changes in different samples. Finally, calculated rates were converted to areal rates using measured surface areas.

Figure 9 shows results for all samples, plotted as a function of average volume radius for each distribution. It may be questionable to use a single size parameter to correlate properties that depend upon distribution. Luss has pointed out the danger of this (*37*). However, scatter in the data does not permit any more definitive analysis. Attempts to determine precise size dependence through solution of equations involving the distribution parameter were unsuccessful. The trends shown in Fig. 9, however, are sufficiently accurate to indicate qualitative features.

Cyclohexane dehydrogenation and benzene hydrogenolysis both increase with increasing crystallite size. The correlations are highly significant and both show a relative increase in rate of 1.96 when the size changes from 2 to 4 nm. This suggests a common intermediate adsorbed on a face plane, such as (111) or (100). The most logical is the (111) plane which has the correct hexagonal structure compatible with six-point adsorption in the plane of the ring. Figure 1 shows only an increase by a factor of 1.11 in going from 2 to 4 nm. However, if (111) plane adsorption is applicable, then an ensemble of seven neighbor atoms is re-

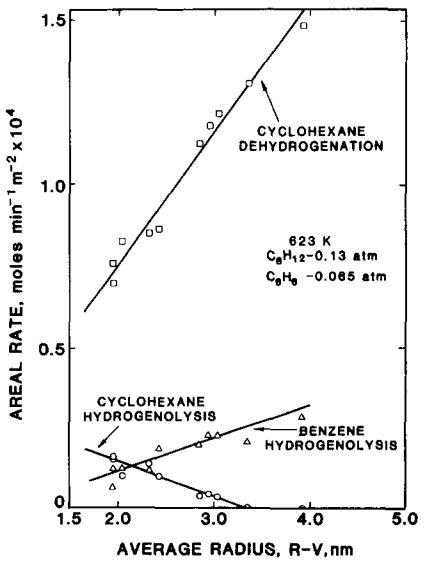

FIG. 9. Effect of crystallite size on reaction rates.

quired. The rate is predicted to increase by a fraction of 1.11 raised to the power of 7 (*38*), which is 2.09, remarkably close to the observed 1.96.

Cyclohexane hydrogenolysis, however, decreases as the size increases. This implies that the reaction is favored over edge-type sites. With two-point adsorption, theory predicts a decrease by a factor of 0.48 for size increases from 2 to 3 nm. This compares favorably with the observed 0.52.

In spite of the oversimplification of a perfect cubo-octahedral crystallite representing surface site concentration of a complex distribution, consistency of these results prompt us to suggest a mechanism in which cyclohexane adsorbs like benzene on face sites with multiple-point adsorption (*38*). Dehydrogenation in this mode gives benzene which then undergoes hydrogenolysis. Cyclohexane hydrogenolysis occurs via the chair-on boat-form with two-point adsorption on the edge sites.

Blakely and Somorjai have expressed similar conclusions based on high-vacuum measurements on single crystal platinum surfaces at 423 K (*38*). These authors found that cyclohexane hydrogenolysis was directly proportional to the density of "step" and "kink" sites, corresponding to the assignment of edge sites invoked in this report. Cyclohexane dehydrogenation was independent of step and kink sites and no dependence or face or plane sites was reported. This is not to be expected at large crystal dimensions where Fig. 1 predicts independence with size. In spite of the difficulty in comparing measurements on platinum single crystals with dispersed nickel catalysts, the findings of Blakely and Somorjai are consistent with those developed here, where we give "edge" sites the same function as "step and kink" sites.

In a previous communication (*30*) we reported excessive loss of surface area in these catalysts as the crystallite size increases due to decreasing accessibility. For example, in going from 2 to 4 nm the accessible surface, defined as the ratio of measured to calculated surface area, decreased by a fraction of about 2. Presumably, the areal rates in Fig. 9 reflect this accessible surface. If the decrease in accessibility is due to complete trapping of crystallites in smaller pores thus removing their surface from reaction, then the areal rates more correctly represent the activity of larger crystallites. Since volume-average radius favors these larger crystallites, similarity of the correlation in Fig. 9 to monodispersed crystallites is rationalized.

From a practical point-of-view, these conclusions indicate a maximum cyclohexane dehydrogenation rate on a catalyst volume basis at a crystallite size of about 1.0 nm, where increasing areal rate and decreasing dispersion combine to give the optimum. However, at temperatures where the reverse reaction is insignificant, cyclohexane hydrogenolysis is high for this size and yields of benzene are low. A better solution is to decrease cyclohexane hydrogenolysis by increasing the crystallite size while maintaining volume conversion with larger nickel loadings. Selectivity of benzene hydrogenolysis to cyclohexane dehydrogenation is essentially invariant with size and cannot be controlled. In this case, benzene yield is best optimized through reactor design and control of operating conditions, temperature, pressure, and space velocity.

We have interpreted these results solely on the basis of size-dependent surface site statistics. Kramer and Zuegg (*40*) have recently suggested on alternate approach in which the interface between Pt and Al_2O_3 plays a role in altering the nonspecific hydrogenation of methyl cyclopentane to *n*-hexane. This "adliniation" is also a possibility here, especially since inaccessibility increases with crystallite size. If this is due to "patches" of SiO_2 covering the nickel, then the metal–support interface between will undoubtedly also increase. However, at this time we are unable to speculate on a

mechanism whereby hydrogenolysis is decreased and dehydrogenation increased as the boundary grows.

ACKNOWLEDGMENT

We are grateful to the Robert A. Welch Foundation for support of this research.

REFERENCES

1. Boudart, M., "Advances in Catalysis," Vol. 20, p. 153. Academic Press, New York, 1969.
2. Van Hardeveld, R., and Van Montfoort, A., *Surf. Sci.* **4,** 396 (1966).
3. Van Hardeveld, R., and Hartog, F., *Surf. Sci.* **15,** 189 (1969).
4. Bond, G. C., *in* "Proceedings, 4th International Congress on Catalysis, Moscow, 1968" (B. A. Kazansky, Ed.). Adler, New York, 1968.
5. Bond, G. C., *Discuss. Faraday Soc.* **41,** 200 (1966).
6. Kobayashi, M., and Shirasaki, T., *J. Catal.* **39,** 148 (1975).
7. Wu, J. C., and Harriott, P., *J. Catal.* **39,** 395 (1975).
8. Darling, T. A., and Moss, R. L., *J. Catal.* **5,** 111 (1967).
9. Oliver, R. G., Wells, P. B., and Grant, J., *in* "Proceedings, 5th International Congress on Catalysis, Palm Beach, 1972" (J. W. Hightower, Ed.). North-Holland, Amsterdam, 1972.
10. Coenen, J. W. E., Vanmeerten, R. Z. C., and Rijnten, M. T., *in* "Proceedings, 5th International Congress on Catalysis, Palm Beach, 1972" (J. W. Hightower, Ed.). North-Holland, Amsterdam, 1972.
11. Cece, J. M., and Gonzalez, R. D., *J. Catal.* **28,** 254 (1973).
12. Delaney, J. E., and Manogue, W. H., *in* "Proceedings, 5th International Congress on Catalysis, Palm Beach, 1972" (J. W. Hightower, Ed.). Elsevier, New York, 1973.
13. Brunelle, J. P., Sugier, A., and Le Page, J. F., *J. Catal.* **43,** 273 (1976).
14. Hanson, F. V., and Boudart, M., *J. Catal.* **53,** 56 (1978).
15. Nieuwenhuys, B. E., and Somorjai, G. A., *J. Catal.* **46,** 259 (1977).
16. Martin, G. A., and Salmon, J. A., *C. R. Acad. Sci., Paris Ser. C* **286,** 127 (1978).
17. Guilleux, M. F., Dalmon, J. A., and Martin, G. A., *J. Catal.* **62,** 235 (1980).
18. Coenen, J. W. E., Schats, W. M. T. M., and Van Meerten, R. Z. C., *Bull. Soc. Chim. Belg.* **88,** 435 (1979).
19. Lam, Y. L., and Sinfelt, J. H., *J. Catal.* **47,** 319 (1976).
20. Fuentes, S., and Figureas, F., *J. Catal.* **61,** 443 (1980).
21. Vannice, M. A., *J. Catal.* **44,** 152 (1976).
22. Vannice, M. A., *J. Catal.* **40,** 129 (1975).
23. Bhatia, S., Bakhshi, N. N., and Mathews, J. F., *Canad. J. Chem. Eng.* **56,** 575 (1978).
24. Dalmon, J. A., and Martin, G. A., *in* "Proceedings, 7th International Congress on Catalysis, Tokyo, 1980," p. A27-1. Elsevier, Amsterdam, 1981.
25. Bartholomen, C. H., Pannell, R. B., Butler, J. L., *J. Catal.* **65,** 335 (1980).
26. Richardson, J. T., and Dubus, R. J., *J. Catal.* **54,** 207 (1978).
27. Huang, P. C., and Richardson, J. T., *J. Catal.* **52,** 332 (1978).
28. Van Meerten, R. Z. C., Habets, H. M. J., Beaumont, A. H. G. M., and Coenen, J. W. E., *in* "Proceedings, 7th International Congress on Catalysis, Part B. Tokyo, 1980," p. 1441. Elsevier, Amsterdam, 1981.
29. Richardson, J. T., Dubus, R. J., Crump, J. G., Desai, P., Osterwalder, U., and Cale, T. S., "Preparation of Catalysts, II," p. 131. Elsevier, Amsterdam, 1979.
30. Desai, P. J., and Richardson, J. T., "Catalyst Deactivation," p. 149. Elsevier, Amsterdam, 1980.
31. Richardson, J. T., and Desai, P. H., *J. Catal.* **42,** 294 (1976).
32. Linsen, B. G., "Physical and Chemical Aspects of Adsorbents and Catalysts." Academic Press, New York, 1970.
33. Ross, R. A., and Valentine, J. H., *J. Catal.* **2,** 39 (1963).
34. Vishwanathan, V. N., and Yeddanappali, L. M., *Z. Anorg. Allg. Chem.* **407,** 62 (1974).
35. Kehoe, J. P. G., and Putt, J. B., *J. Appl. Chem. Biotechnol.* **22,** 23 (1972).
36. Rohrer, J. E., and Sinfelt, J. H., *J. Phys. Chem.* **66,** 1190 (1962).
37. Luss, D., *J. Catal.* **23,** 119 (1971).
38. Rideal, E. K., "Concepts in Catalysis." Academic Press, New York/London, 1968.
39. Blakely, D. W., and Somorjai, G. A., *J. Catal.* **42,** 181 (1976).
40. Kramer, R., and Zuegg, H., *J. Catal.* **80,** 446 (1983).